AAS 10-xxx

SHIFTING THE INERTIAL NAVIGATION PARADIGM WITH MEMS TECHNOLOGY

Timothy P. Crain II *, Robert H. Bishop †, and Tye Brady ‡

"Why don't you use MEMS?" is of the most common questions posed to navigation systems engineers designing inertial navigation solutions in the modern era. The question stems from a general understanding that great strides have been made in terrestrial MEMS accelerometers and attitude rate sensors in terms of accuracy, mass, and power. Yet, when compared on a unit-to-unit basis, MEMS devices do not provide comparable performance (accuracy) to navigation grade sensors in several key metrics. This paper will propose a paradigm shift where the comparison in performance is between multiple MEMS devices and a single navigation grade sensor. The concept is that systematically, a sufficient number of MEMS sensors may mathematically provide comparable performance to a single navigation grade device and be competitive in terms power and mass allocations when viewed on a systems level. The implication is that both inertial navigation system design and fault detection, identification, and recovery could benefit from a system of MEMS devices in the same way that swarm sensing has benefited Earth observation and astronomy. A survey of the state of the art in inertial sensor accuracy scaled by mass and power will be provided to show the *scaled error* in MEMS and navigation graded devices, a mathematical comparison of multi-unit to single-unit sensor errors will be developed, and preliminary application to an Orion lunar skip atmospheric entry trajectory will be explored.

INTRODUCTION

Section content (list to be removed in final version):

- restate concept from abstract
- introduce concept of multi-sensor/single-functional (MSSF) FDIR paradigm
- introduce concept of swarm sensing
- explain how the swarm can compete with the MSSF approach once all aspects are considered

The simplest answer to the hypothetical question asked in the abstract, "Why don't you use MEMS?", is that in a unit-to-unit comparison MEMS inertial sensing technology is at least an order of magnitude less accurate than navigation and strategic grade sensors. If the accuracy from these high grade devices (discussed in the following section in comparison to MEMS devices) is required for vehicle level navigation accuracy then MEMS are typically not considered in the early formulation phases of a project. Consider the generalized spacecraft navigation system presented in Figure 1 where onboard sensors such as Global Positioning System (GPS) receivers, inertial measurement units (IMUs), and altimeters are used in conjunction with external navigation updates to support the operation of guidance and control algorithms. In applications such as human spaceflight where robustness and reliability are navigation priorities a multi-sensor, single functionality (MSSF) approach is often employed where a small number of IMUs are employed to provide enough cross-checking information to ensure that at least one functional unit is available for processing by the navigation algorithms. In the MSSF approach, the navigation solution provided to guidance and control

*Aerospace Engineer, NASA - Johnson Space Center, Houston TX 77058, Member AAS, Member AIAA.
†Department Chair, Aerospace Engineering Department, The University of Texas at Austin, TX 78759-5321. Member AAS, Associate Fellow AIAA.
‡Some dude at Draper.

will use one and only one IMU based upon the FDIR and selection algorithms. The number of IMUs would be determined by the desired depth of unit fault tolerance and a probabilistic evaluation of critical mission phases. An example of an MSSF architecture is provided in Figure 2.

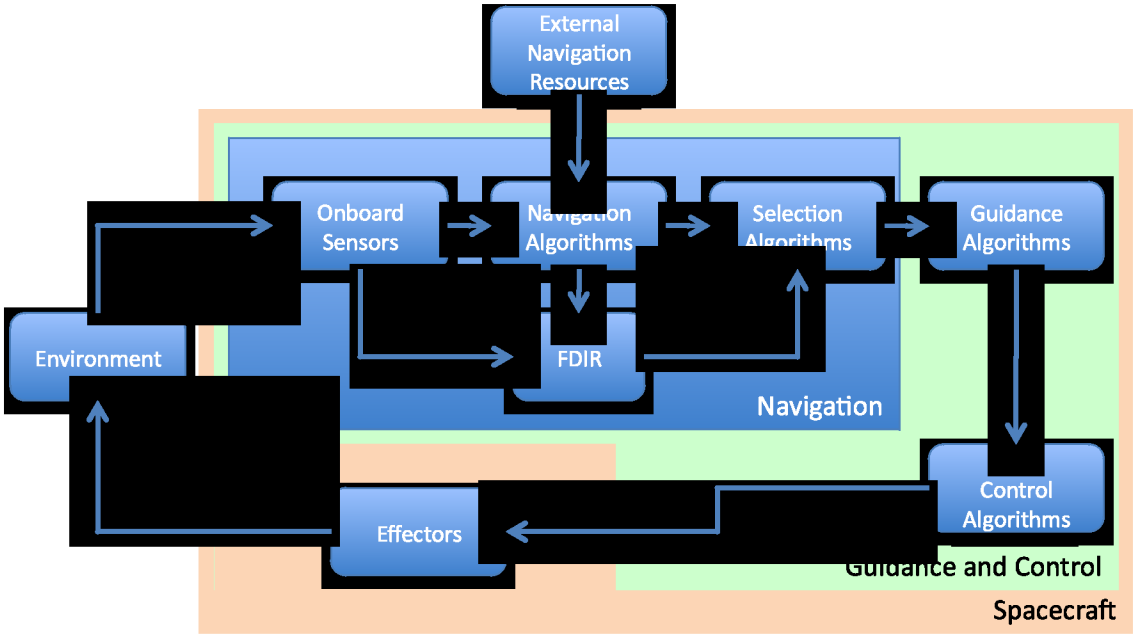

Figure 1 General Navigation Flow

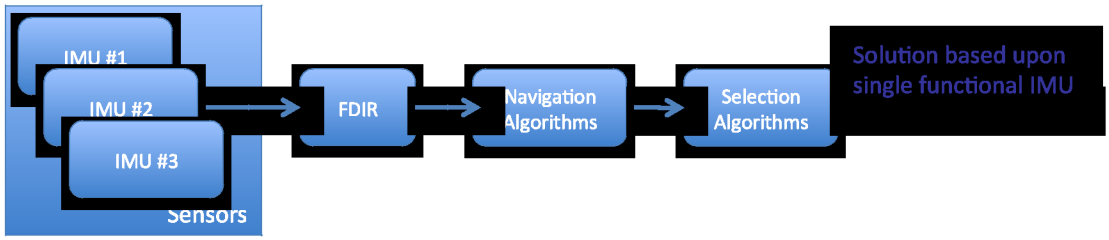

Figure 2 Multi-Sensor Single Function (MSSF) Example

Swarm sensing borrows from the paradigm employed by large sensor arrays and employs a larger number of IMUs with less accuracy to provide robustness and sufficient uncorrelated measurements to compensate for the error inherent in each sensor. This approach, illustrated in Figure 3, will employ a sensor management module to combine the N outputs from the swarm into a single synthetic measurement for processing by the navigation algorithm. While the sensor manager may de-weight or eliminate the output from poorly performing IMUs, it is unlike the FDIR and sensor selection modules in the MSSF paradigm because it does not necessarily try to select a single IMU output for the navigation algorithm.

This paper will specifically address two questions:

- Can a sufficient number of MEMS IMUs be employed in a swarm to provide an data with accuracy equivalent to a single navigation grade IMU in an MSSF paradigm?
- Is there a systematic level benefit in mass, power, and robustness to employing a MEMS sensor swarm?

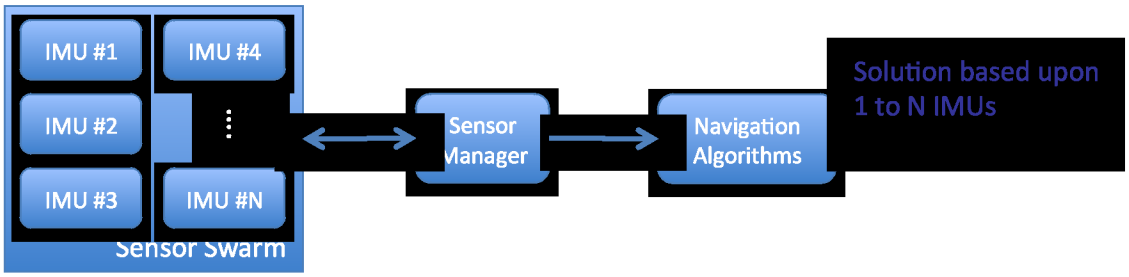

Figure 3 Sensor Swarm Example

The latter question can be answered even in the context of a MEMS swarm that does not quite duplicate the accuracy of a navigation grade IMU and MSSF system.

SURVEY

Section content (list to be removed in final version):

- List 5 representative IMUs and their characteristics: MEMS1, MEMS2, Tactical, Navigation, Strategic
- discuss future of sensors in this area (evolutionary vs. revolutionary changes expected)

As a reference for each of these classes of IMUs, a Northrup Grumman SIRU* , a Honeywell MIMU[†], a Northrup Grumman LN-200S[‡], a Draper ISC[§], and an advanced Draper ISC MEMS[¶] are provided with representative specifications and mass, power, volume budgets.

ANALYTIC COMPARISON

Section content (list to be removed in final version):

- develop error metric for IMUs
- introduce concept of "error-mass"
- introduce concept of "error-power"
- show how both of these vary for the MSSF and swarm approaches on a trend plot
- develop simplified error equations for swarm error

Accelerometer Model

The measurement of the non-gravitational acceleration at the IMU is corrupted by errors due to nonorthogonality and misalignment of the axes, $\mathbf{\Gamma}_a$, errors due to scale-factor uncertainties, $\mathbf{S}_a$, random biases, $\mathbf{b}_a$, and noise, $\boldsymbol{\eta}_a$.

The measured non-gravitational acceleration, $\mathbf{a}_{ng,m}$, can be written in terms of the true non-gravitational acceleration, $\mathbf{a}_{ng}$, as

*Accelerometer option included. Performance of accels quoted from NEAR spacecraft.
[†]Accels performance from 1999 data sheet.
[‡]Space grade version of LN200.
[§]M/P/V includes star camera and accel board. Accels based on MMIMU data.
[¶]M/P/V includes star camera and accel board. Accels based on MMIMU data.

Table 1 Representative IMU Accuracy Specifications and Physical Characteristics

Value		Strategic	Navigation	Tactical	MEMS	MEMS+
Example HW		SIRU	MIMU	LN200S	ISC	ISC-A
Reference		[1], [2], [3]	[4], [9], [10]	[5]	[6], [7]	[6], [7]
Accel (1σvalues)						
Bias	micro-G	50	100	300	2000	2000
Scale Factor	PPM	175	175	300	600	600
Non-ortho	micro-rad	70	70	100	1000	1000
Noise	micro-G	10	100	35	100	100
Gyro (1σvalues)						
ARW	deg/rt-hr	0.00001	0.005	0.07	0.16	0.01
Scale Factor	PPM	1.5	1	100	100	30
Non-ortho	micro-rad	175	170	100	100	100
Bias Stability	deg/hr	0.0003	0.005	1	3.3	1
Budgets						
Mass	kg	7.1	10.5	0.75	2.9	1.9
Volume	cu cm	7751	7147	529	2234	1050
Power	W	38	42	12	3.6	3.5

$$\mathbf{a}_{ng,m} = (\mathbf{I} + \mathbf{\Gamma}_a)(\mathbf{I} + \mathbf{S}_a)(\mathbf{a}_{ng} + \mathbf{b}_a + \boldsymbol{\eta}_a) \,,$$

where $\boldsymbol{\eta}_a$ is a zero-mean stochastic process with

$$\mathrm{E}\left\{\boldsymbol{\eta}_a(t)\boldsymbol{\eta}_a^{\mathrm{T}}(\tau)\right\} = \mathbf{Q}_a\delta(t-\tau)\,.$$

The form of the nonorthogonality/axes-misalignment matrix and the scale-factor uncertainty matrix is such that

$$\mathbf{\Gamma}_a = \begin{bmatrix} 0 & \gamma_{a,xz} & -\gamma_{a,xy} \\ -\gamma_{a,yz} & 0 & \gamma_{a,yx} \\ \gamma_{a,zy} & -\gamma_{a,zx} & 0 \end{bmatrix} \text{ and } \mathbf{S}_a = \begin{bmatrix} s_{a,x} & 0 & 0 \\ 0 & s_{a,y} & 0 \\ 0 & 0 & s_{a,z} \end{bmatrix}.$$

For the purposes of this paper, we are primarily concerned with the instantaneous error on each accelerometer

$$\begin{aligned} \mathbf{e}_a &= \mathbf{a}_{ng,m} - \mathbf{a}_{ng} && (1)\\ &= (\mathbf{I} + \mathbf{\Gamma}_a)(\mathbf{I} + \mathbf{S}_a)(\mathbf{a}_{ng} + \mathbf{b}_a + \boldsymbol{\eta}_a) - \mathbf{a}_{ng} && (2)\\ &\approx (\mathbf{I} + \mathbf{\Gamma}_a + \mathbf{S}_a)(\mathbf{a}_{ng} + \mathbf{b}_a + \boldsymbol{\eta}_a) - \mathbf{a}_{ng} && (3)\\ &\approx (\mathbf{\Gamma}_a + \mathbf{S}_a)\,\mathbf{a}_{ng} + (\mathbf{b}_a + \boldsymbol{\eta}_a) && (4) \end{aligned}$$

Gyroscope Error Model

The measurement of the angular velocity of the spacecraft is corrupted by errors due to nonorthogonality and misalignment of the axes, $\mathbf{\Gamma}_g$, errors due to scale-factor uncertainties, $\mathbf{S}_g$, random biases, $\mathbf{b}_g$, and noise, $\boldsymbol{\eta}_g$.

The measured angular velocity, $\boldsymbol{\omega}_m$, can be written in terms of the true angular velocity, $\boldsymbol{\omega}$, as

$$\boldsymbol{\omega}_m = (\mathbf{I} + \mathbf{\Gamma}_g)(\mathbf{I} + \mathbf{S}_g)(\boldsymbol{\omega} + \mathbf{b}_g + \boldsymbol{\eta}_g) \ ,$$

where $\boldsymbol{\eta}_g$ is a zero-mean stochastic process with

$$\mathrm{E}\left\{\boldsymbol{\eta}_g(t)\boldsymbol{\eta}_g^{\mathrm{T}}(\tau)\right\} = \mathbf{Q}_g\delta(t-\tau) \, .$$

For the purposes of this study, a representative attitude error is desired as a metric and the error after 30 minutes of propagation on the gyros ($\mathbf{e}_{pg} = \int \mathbf{e}_g(t)dt$) will be assumed rather than the instantaneous gyro attitude rate error ($\mathbf{e}_g = \omega_m - \omega$). The rationale for this time interval is that 30 minutes provide adequate time for both entry, descent, and landing and transient adverse orbital lighting when star tracker attitude updates are not available. Therefore, the attitude error induced by gyro data processing will be modeled as

$$\mathbf{e}_g \approx \left[(\mathbf{\Gamma}_g + \mathbf{S}_g)\,\omega_{\mathbf{test}} + \mathbf{b}_g + \frac{\boldsymbol{\alpha}_g}{\sqrt{\Delta t}}\right]\Delta t \tag{5}$$

where $\omega_{\mathbf{test}}$ is a test true attitude rate utilized to drive scale factor and orthogonality error inputs, $\boldsymbol{\alpha}_g$ is the angle random walk of the gyro in terms of $deg/rt - hr$, and Δt is the 30 minute error sample interval.

MSSF vs. Swarm Navigation System Errors

Primary sensor performance in an MSSF system is typically not realized because of FDIR thresholds. This is a direct result of the purpose of an MSSF system to use N-1 sensors to assure that one primary sensor is operating within specifications but has some margin to prevent rapid switching between primary sensors. For example, assume that failure detection thresholds are set at τ times the 1σ error characteristic of an inertial sensor

$$\sigma_{eff} = \tau\sigma_{spec} \tag{6}$$

The value of τ may quickly exceed 4 for guaranteed performance in an MSSF, in other words it is possible to select a sensor that is slightly out of spec for generation of the primary navigation solution.

The swarm sensor paradigm incorporates all data available and should guarantee a reduction compared to the single unit error specification equivalent to

$$\sigma_{eff} = \frac{3\sigma_{spec}}{\sqrt{N}} \tag{7}$$

Examination of Figure 4 illustrates that after $N = 10$ the effective reduction in per unit error has reached a point of diminishing returns in terms of improving accuracy. However, this also indicates that single unit failures in a swarm system with 10 to 15 units will not adversely affect overall performance.

The first question that this paper addresses is that of when does a swarm of N sensors provide equivalent performance to a single navigation grade sensor in an MSSF system:

$$\sigma_{eff/s} = \sigma_{eff/MSSF} \tag{8}$$

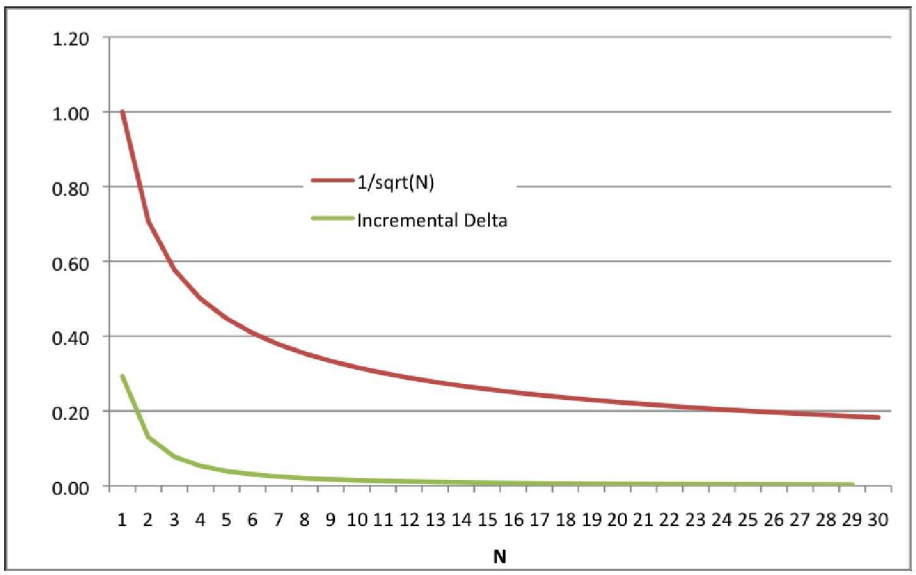

Figure 4 Conceptual Error Reduction from Swarm of N Sensors

or equivalently

$$\frac{3\sigma_{spec,s}}{\sqrt{N}} = \tau\sigma_{spec,MSSF} \tag{9}$$

Solving for N

$$N = \left(\frac{3\sigma_{spec,s}}{\tau\sigma_{spec,MSSF}}\right)^2 \tag{10}$$

if we let R represent the performance ratio between the swarm sensor and the MSSF sensor spec error characteristics

$$R = \frac{\sigma_{spec,s}}{\sigma_{spec,MSSF}} \tag{11}$$

then

$$N = \left(\frac{3R}{\tau}\right)^2 \tag{12}$$

or

$$R = \frac{\tau}{3}\sqrt{N} \tag{13}$$

The final form of this relationship is plotted in Figure 5 for various values of N. Using the rule of thumb that $N = 10$ swarm sensors provide a practical limit in effective accuracy, the middle line marked with 'x' data points provides the relationship between performance ratio R and MSSF threshold τ for inertial accuracy equivalence. For example, a swarm sensor inertial navigation system with 10 units, and a performance ratio of 5, will match the assured accuracy of an MSSF system with a FDIR threshold of $5\sigma_{spec,MSSF}$.

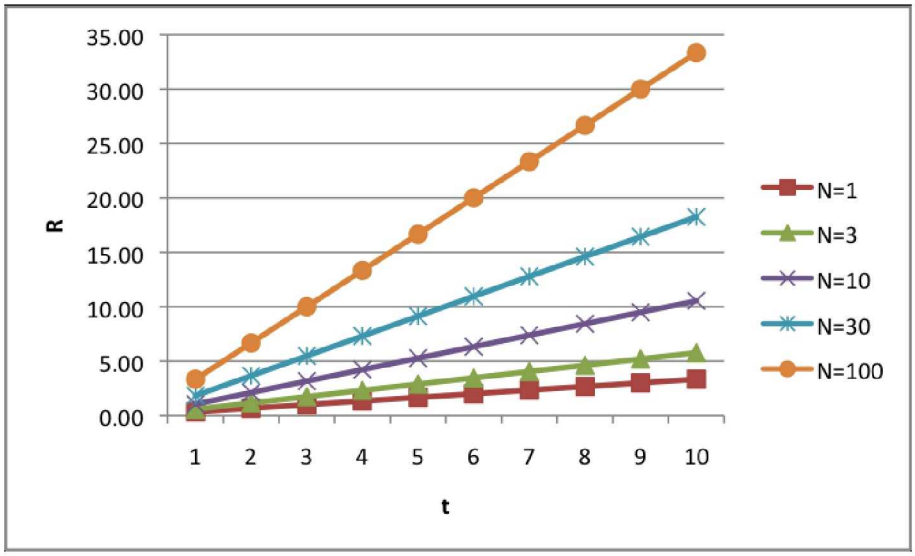

Figure 5 Plots of Constant N: Performance Ratio versus MSSF Threshold

Applying the error characteristic equations developed in Equations 4 and 5 to the representative error specifications, mass, and power in Table 1 provides the single unit error characteristics in Table 2. The points of interest in this table are that ..... to complete this section once Tye confirms representative characteristics table

Table 2 Single Unit Error, Error*Mass, and Error*Power Characteristics

Value	Strategic	Navigation	Tactical	MEMS	MEMS+
Error					
Accel (μg)	305.0	445.0	735.0	3700.0	3700.0
Gyro (deg@30 minutes)	0.953	0.929	1.63	2.84	1.2
Error*Mass					
Accel (μg-kg)	2165.5	2091.5	551.3	10730.0	7030.0
Gyro (deg-kg)	6.768	4.368	1.22	8.25	2.3
Error*Power					
Accel (μg-W)	11590.00	9790.0	8820.0	13320.0	12950.0
Gyro (deg-W)	36.224	20.448	19.55	10.24	4.23

Taking the performance characteristics for accelerometers R_{accel} and R_{gyro} with respect to the representative navigation grade IMU generates the values in Table 3. These values predict that the MEMS and MEMS+ can be employed in a swarm sensor paradigm for both translation and attitude navigation per Equation 13 with swarms of 10 sensors and MSSF thresholds of 5. The tactical grade IMUs would be acceptable for acceleration sensing, but the higher level of attitude error would indicate it is not as well suited overall for a swarm sensing application.

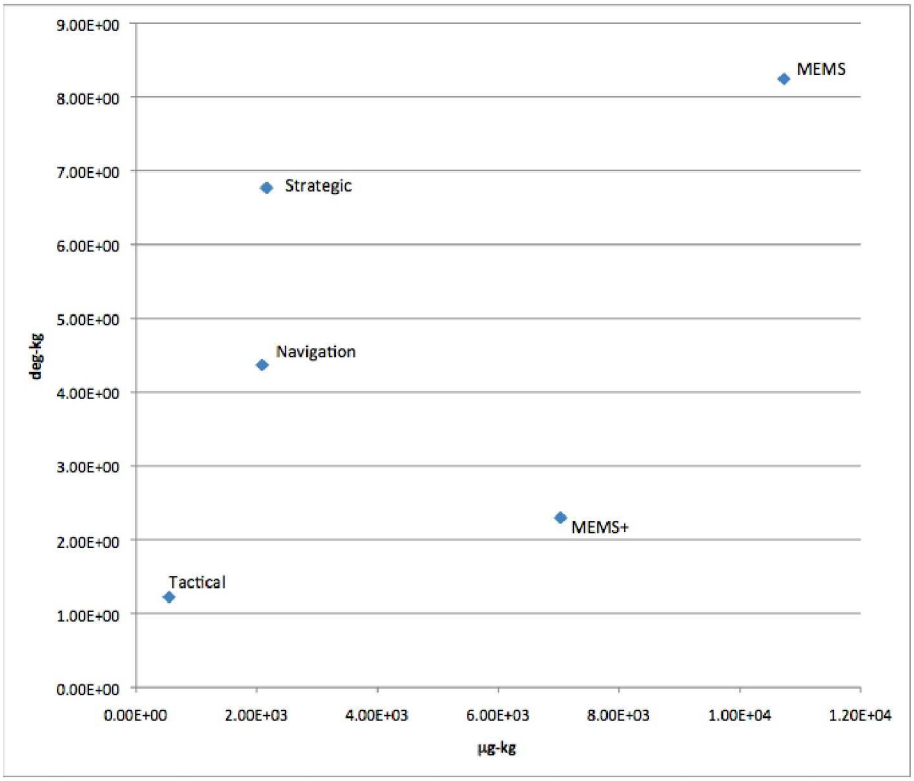

Figure 6 IMU Accuracy Scaled By Mass

Table 3 Performance Ratios Relative to Representative Navigation Grade IMU

Value	Strategic	Navigation	Tactical	MEMS	MEMS+
R_{accel}	0.685	1.00	1.65	8.31	8.31
R_{gyro}	1.026	1.00	1.75	3.06	1.30

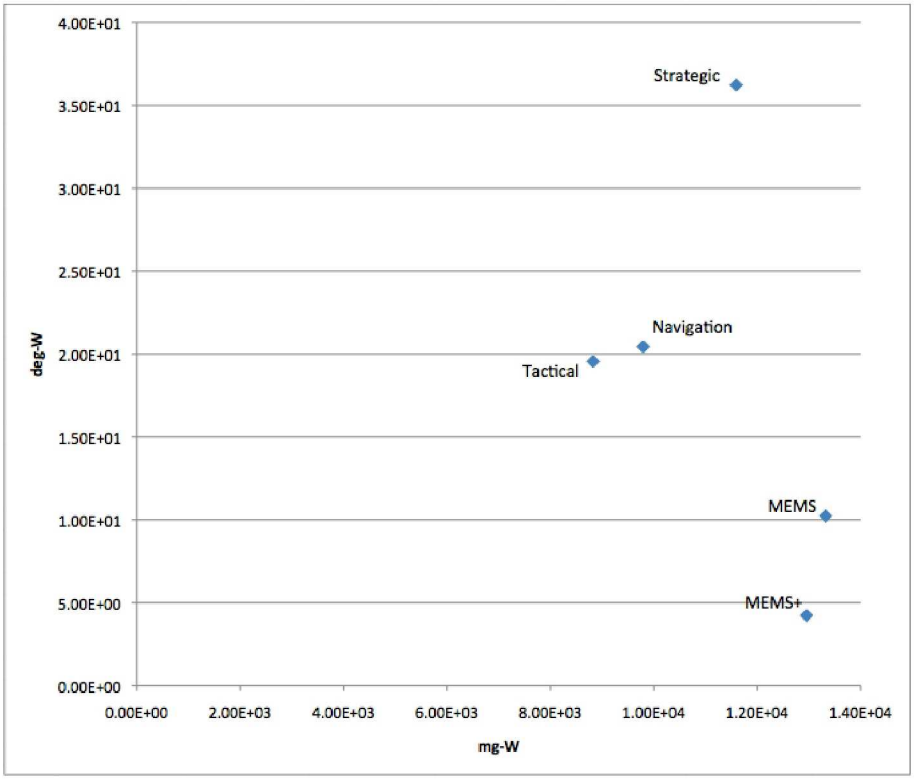

Figure 7 IMU Accuracy Scaled By Power

APPLICATION TO LUNAR RETURN ENTRY NAVIGATION

Section content (list to be removed in final version):

- introduce Orion skip entry trajectory
- compare monte carlo results of true measurements vs. MIMU MSSF, N unit swarm

It is the authors' opinion that atmospheric entry navigation represents the driving scenario for accuracy and robustness in human spaceflight. In this regime, attitude updates are unlikely and translation state updates dependent on communications. Therefore, an Orion lunar return skip entry trajectory [8] will be used as comparison application of a traditional MIMU MSSF based navigation system and a swarm paradigm MEMS+ navigation system. The duration of the trajectory is slightly over 27 minutes long and experiences a variety of translation and attitude regimes as illustrated in Figures 8 and 9. For this analysis, 4 units are assumed in the MIMU MSSF configuration to provide complete isolation of 2 soft failures (operation beyond spec, but within reason) and isolation of 3 hard failures. Published MIMU accuracies are used with the updated estimates for Orion IMU mass and power. To allow for fault detection thresholds, a τ of 5 is assumed in this system per Equation 6. By comparison, a 15 unit MEMS+ swarm is assumed to maximize accuracy while still providing up to 5 unit failures without noticeable effect on overall performance per 4. The mass and power for these systems are summarized in Table 4. In this particular comparison, the swarm improves upon the traditional MSSF system mass requirement by almost 14 kg and operates with 112 fewer Watts. An additional benefit of the swarm configuration not explored in this paper is that a subset of the units could be operated during more benign regimes such as orbital coast or during power conservation contingencies for a significantly smaller power requirement.

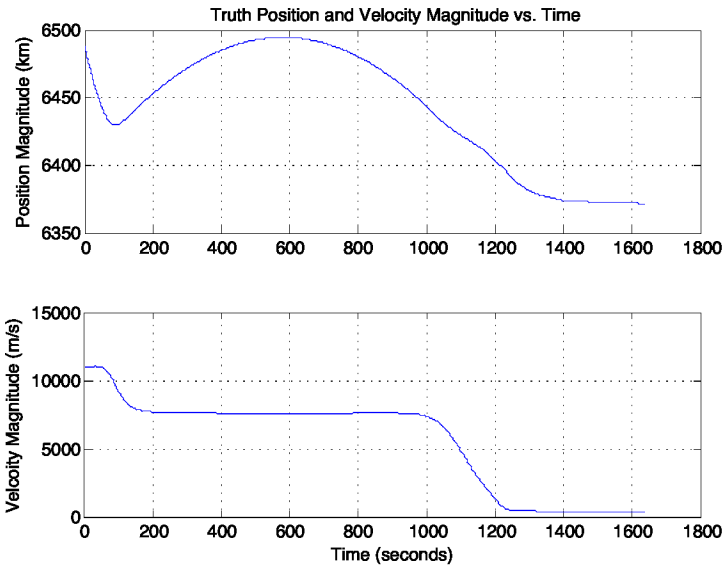

Figure 8 Skip Entry Truth ECI Position and Velocity Time Histories

Table 4 Mass and Power Requirements of MSSF and Swarm Test Cases

	MIMU MSSF	MEMS+ Swarm
No. Units	4	15
Total Mass (kg)	42	28.5
Total Power (W)	168	52.5
τ	5	-
Fault Tolerance	3 hard, 2 soft	5

In this application, the high fidelity skip entry data from Rea [8] is used to drive IMU error models per Equations 1 and 5 at 40 Hz. The IMUs are all assumed to be located at the vehicle center of gravity and aligned with the body axes of the vehicle. A single GPS position and velocity update is assumed at the top of the exoatmospheric arc at approximately 600 seconds in the simulation, but otherwise all navigation translation and inertial attitude states evolve via dead reckoning with a simple fourth order Runge-Kutta integration of a J2 gravity field and the IMU outputs. For the MIMU case, the error specification of a single MIMU was doubled to approximate the effect of τ FDIR thresholds without specifically implementing FDIR software logic. The swarm sensor configuration simply averaged the sensed acceleration and body rate from each unit in the swarm.d

The instantaneous acceleration error characteristics (Equation 4) for both systems as driven by the trajectory data are provided in Figure 10. The signature in the instantaneous error characteristics is the result of the scale factor and non-orthogonality errors amplifying the true sensed acceleration in Figure **??**. Given that the analytic accelerometer characteristic of the MEMS+ device is 8 times as large as the MIMU (see Table 3) the equivalency in error factors is to be expected based upon the $1/\sqrt{15}$ improvement of the swarm averaging and the FDIR threshold effect on the MSSF configuration. The gyro error characteristics based upon a 30 minute time interval at each point in the trajectory is similarly provided in Figure 12. It is in this metric that the value of the swarm is manifest as the indication is that the attitude error (sampled at each instant) would be an order of magnitude smaller than in the case of the MSSF.

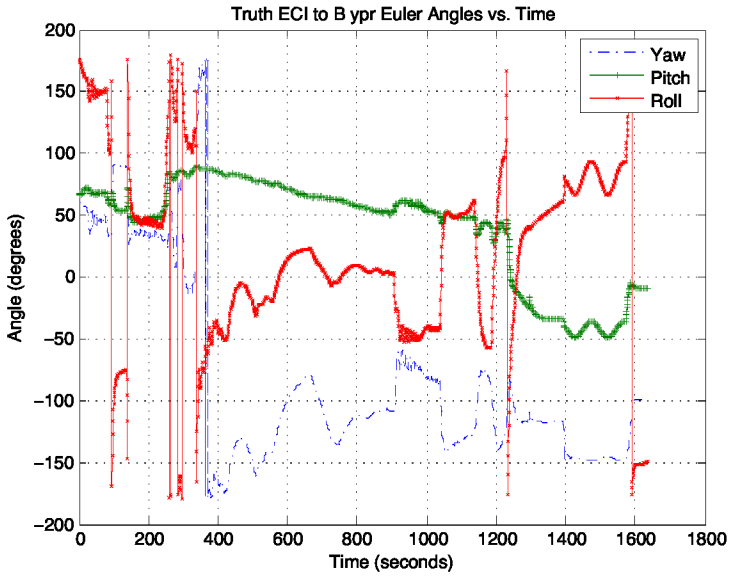

Figure 9 Skip Entry Truth ECI to Body Euler Angle Time Histories

A 100 run Monte Carlo was performed along the reference trajectory for each sensor configuration. The 3σ errors in translation and attitude state propagatoins at each sample time are provided in Figures 15 and 16 for the MIMU MSSF and in Figures 17 and 18 for the MEMS+ swarm. The GPS update is evident at 600 seconds after the first entry pass in the position and velocity errors for both configurations. As expected, in both cases the primary errors in the position are found in the up (U) and alongtrack (V) directions. However, the swarm errors are approximately half those of the MSSF system at the end of the trajectory. It is worth noting that the actual Orion navigation scheme uses a much more sophisticated propagation approach and nominally incorporates GPS whenever available during the trajectory, so the results presented here are conservative in all cases in the estimation of error. Nonetheless, in a comparison of equivalent assumptions the position and velocity accuracy of the swarm system outperforms the MSSF system in this application. The attitude errors in the Euler angles similarly display a nod toward the swarm configuration in terms of accuracy.

CONCLUSION AND FORWARD WORK

Section content (list to be removed in final version):

- discuss results from analytic and numerical studies
- discuss practical limits
- propose future work in field testing

A new paradigm for utilizing inertial sensors has been introduced. While the concept of collecting multiple measurements to reduce systematic, per instrument, error is not novel the application in consideration of balancing mass, power, and fault tolerance does bring a systems engineering perspective to the problem of selecting inertial sensors for an entry vehicle. A static comparison of navigation grade and state-of-the-art MEMS IMUs indicates that it is not practical to match or improve on the navigation grade IMU performance with a swarm of N sensors for acceleration measurement. However, angular rate measurement from a MEMS based swarm system is competitive with a traditional navigation grade IMU system in terms of power at a slightly increased mass. The integrated effect of swarm measurement averaging was shown to improve on the MSSF approach in a highly dynamic, open-loop navigation Monte Carlo simulation of a lunar return skip

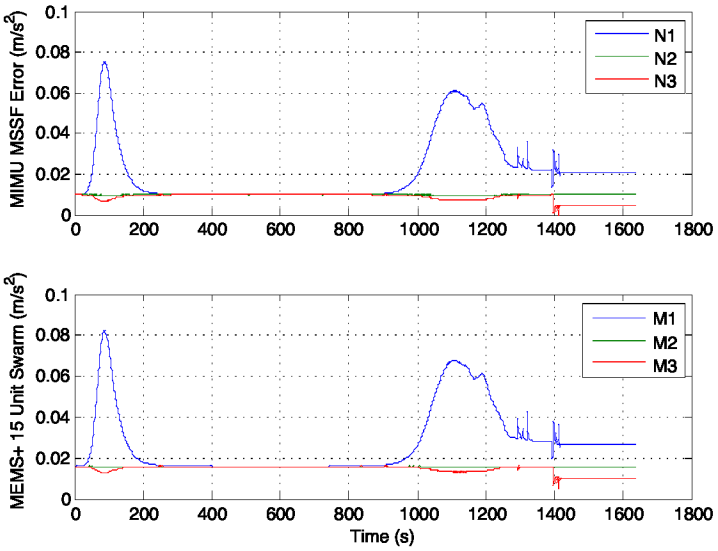

Figure 10 MIMU MSSF to MEMS+ 15 Swarm Accelerometer Error Characteristics

entry. Further work in the areas of fault detection, swarm processing architecture design, analysis in a closed loop GN&C simulation, and extensive field testing remain to prove out the concept of swarm sensing but the paradigm is clearly feasible and warrants further development.

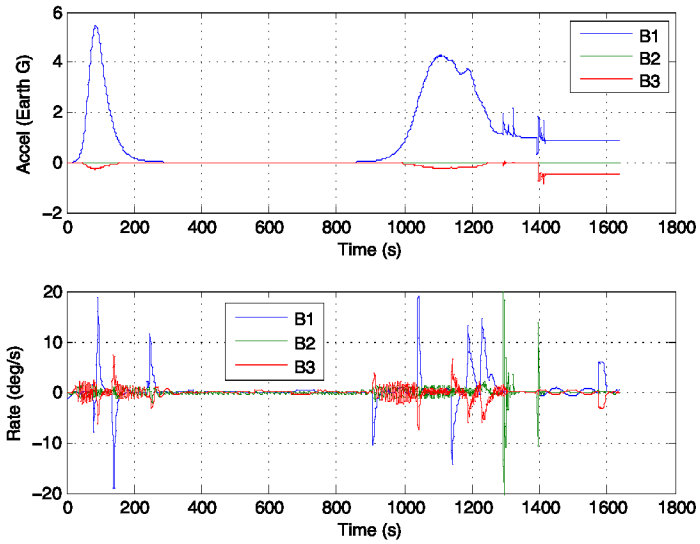

Figure 11 True Sensed Accelerations and Rotation Rates in the Vehicle Body Frame

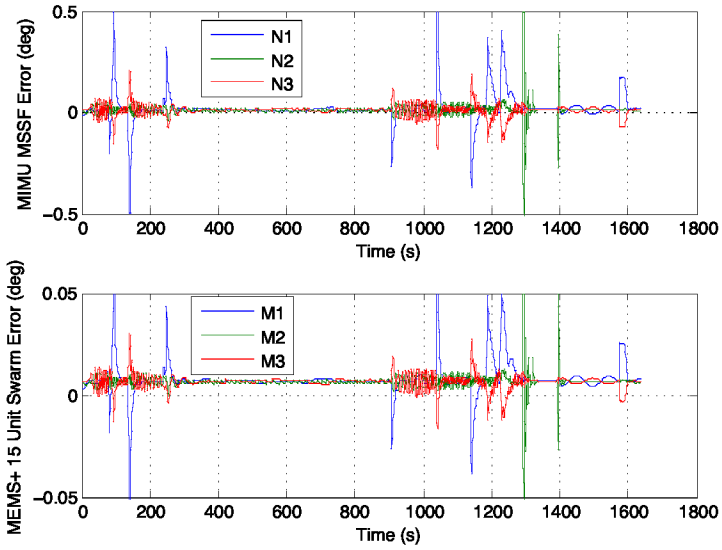

Figure 12 MIMU MSSF to MEMS+ 15 Swarm Gyro Error Characteristics

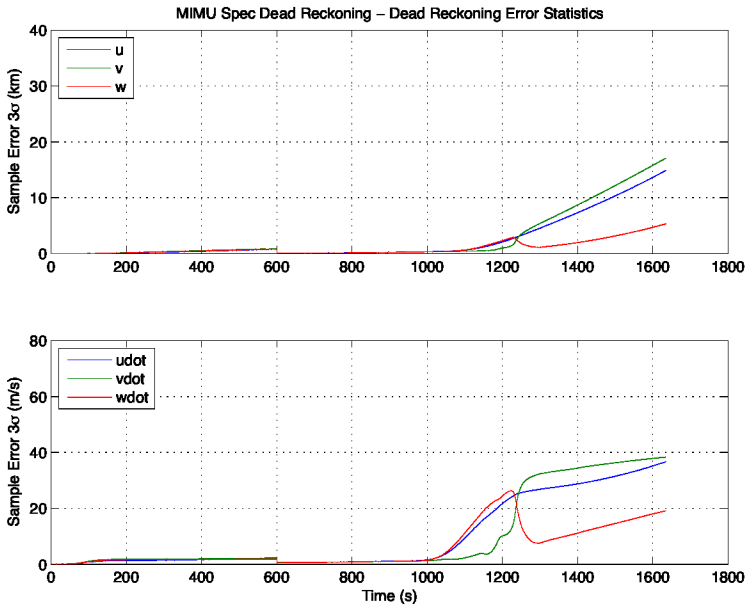

Figure 13 MIMU Spec Spec Position and Velocity Monte Carlo Sample Statistics

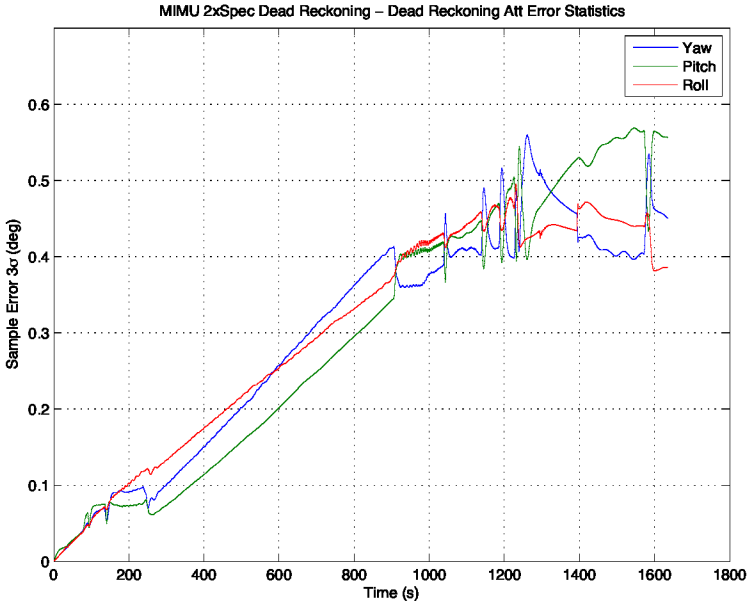

Figure 14 MIMU Spec ECI to Body Euler Angle Monte Carlo Sample Statistics

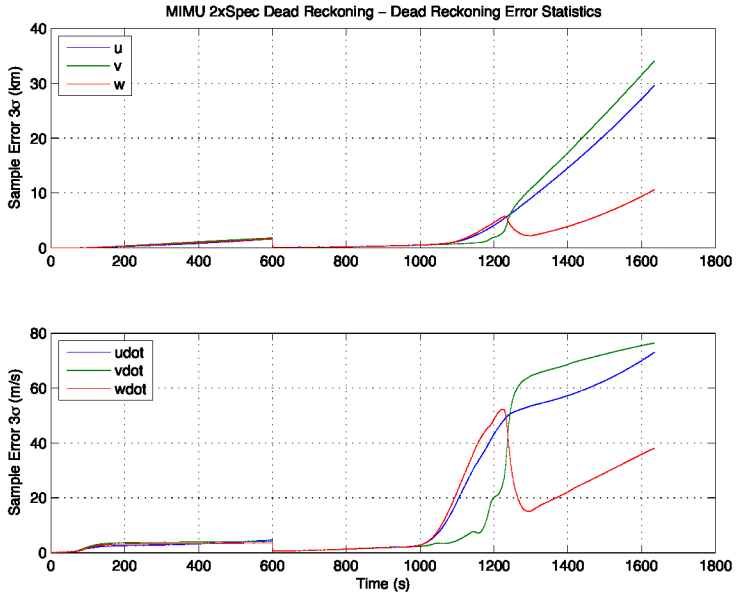

Figure 15 MIMU 2x Spec Position and Velocity Monte Carlo Sample Statistics

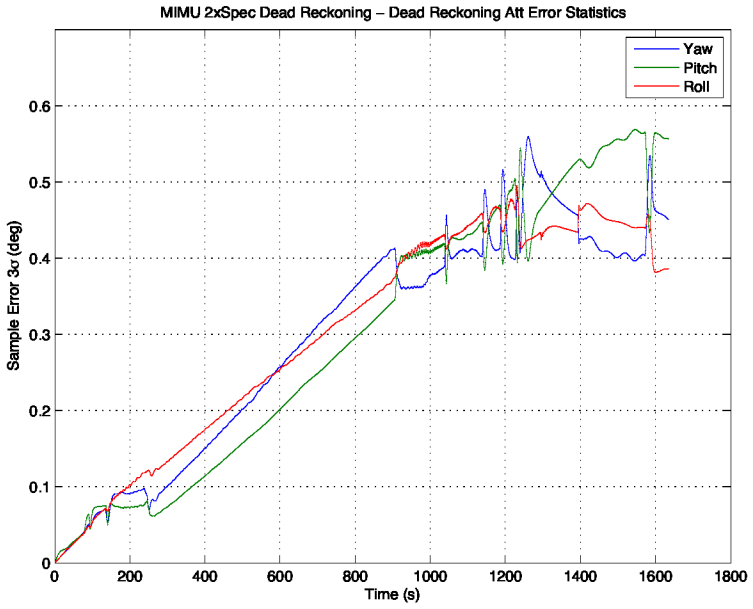

Figure 16 MIMU 2x Spec ECI to Body Euler Angle Monte Carlo Sample Statistics

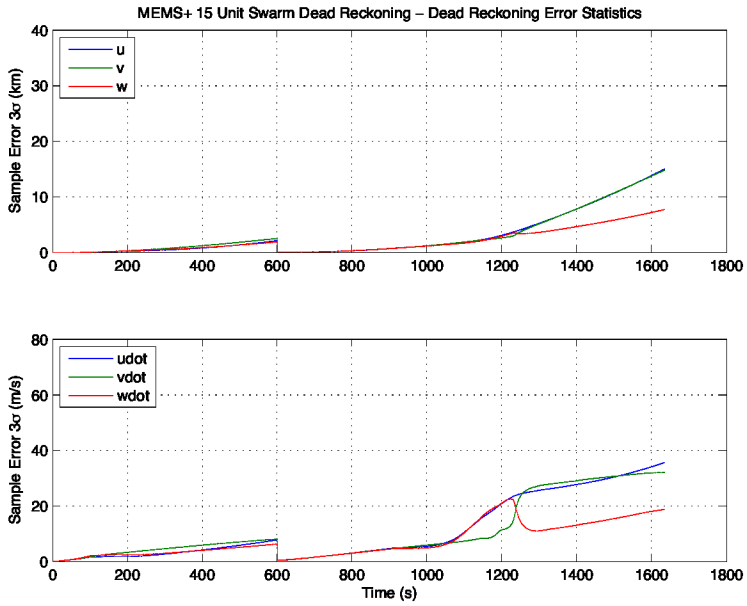

Figure 17 MEMS+ 15 Unit Swarm Position and Velocity Monte Carlo Sample Statistics

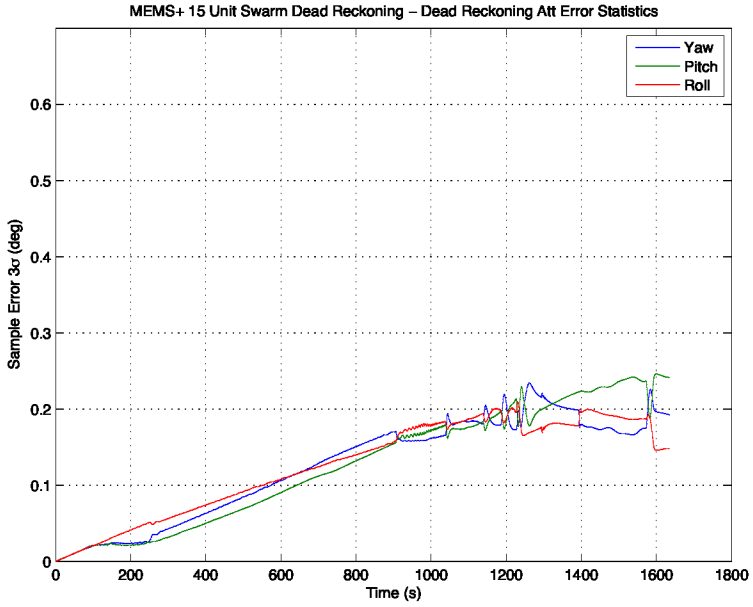

Figure 18 MEMS+ 15 Unit Swarm ECI to Body Euler Angle Monte Carlo Sample Statistics

REFERENCES

[1] Northrop Grumman Data Sheet, http://www.es.northropgrumman.com/solutions/sirudual/assets/scalable_SIRU.pdf

[2] Rozelle, D., "The Hemispherical Resonator Gyro: From Wineglass to the Planets", Space Flight Mechanics Conference, Savannah, Georgia, 8 12 February 2009.

[3] Londerville, G.; Ciolino, R.; Haley, D., "In-Flight Experience of the Space Inertial Reference Unit Utilizing the Solid State HRG", Spacecraft Guidance, Navigation and Control Systems, Proceedings of the 3rd ESA International Conference held 26-29 November, 1996 at ESTEC, Noordwijk, the Netherlands.

[4] Honeywell Data Sheet, http://www51.honeywell.com/aero/common/documents/myaerospacecatalog-documents/MIMU.pdf

[5] Northrop Grumman Data Sheet, http://www.es.northropgrumman.com/solutions/ln200/assets/Inertial_Measurement_Unit_LN-2.pdf

[6] Brady, T., "Next Generation Inertial Stellar Compass", Space Flight Mechanics Conference, Savannah, Georgia, 8 12 February 2009.

[7] Barbour, N., "Inertial MEMS Systems Applicatons", Advances in Navigation Sensors & Integration Technology. London, UK. 10/20/2003 - 10/28/2003.

[8] Jeremy, Rea., "DAC3 POD Entry Trajectories," *Orion Flight Dynamics Team Technical Report* , FltDyn-CEV-09-22, March 2009.

[9] Orion IMU Mass at PDR Reference, TBD

[10] Orion IMU Power at PDR Reference, TBD